JOURNAL OF MATERIALS SCIENCE **36** (2001) 5865–5870

Microstructural development of Ti-24Al-14Nb-3V-0.5Mo alloy during hot tensile deformation

Y. WU
Inha University, Division of Materials Science and Engineering, Incheon, 402-751, Korea; Beijing General Research Institute of Mining and Metallurgy, Beijing 100044, People's Republic of China

S. K. HWANG
Inha University, Division of Materials Science and Engineering, Incheon, 402-751, Korea; Center for Advanced Aerospace Materials, Pohang University of Science and Technology, Pohang, Korea

Microstructure of the Ti-24Al-14Nb-3V-0.5Mo (at.%) alloy deformed from room temperature to 700°C was studied by the H-800 transmission electron microscope (TEM) equipped with a side entry goniometer stage capable of ±45° tilt on the *X* or *Y* axis operating under two-beam condition. Especially dislocation types and slip systems of the α_2-phase ($D0_{19}$) were analyzed in accordance with $\vec{g}\cdot\vec{b}=0$ invisibility criterion. The results indicated that with increasing the deformation temperature from room temperature to 700°C, the slip of $\vec{a}$-type dislocations on prismatic planes $\{10\bar{1}0\}$ in the α_2-phase was enhanced whereas that on basal plane (0001) with hexagonal networks morphology was suppressed during tensile deformation. Being immobile, the dislocation networks were thought to be mainly responsible for the low ductility at low temperature. When the test temperature was increased to 700°C, the $\vec{c}+\vec{a}/2$-type dislocation glide on pyramidal planes $\{0\bar{2}21\}$ was also observed, but the hexagonal dislocation networks formed by the slip of $\vec{a}$-type dislocations on basal planes were hardly seen. During the high temperature deformation microstructural refinement was also observed due to dynamic recovery and recrystallization. This, together with the precipitation of secondary α_2 phase and O phase during deformation all contributed to ductility of the present alloy at high temperature.

1. Introduction

Ti_3Al-base alloys have excellent potential as advanced aerospace and high temperature structural materials for their high strength, improved oxidation and creep resistance as well as good elevated temperature strength compared to conventional titanium based alloys [1, 2]. However, their practical applications are limited by their poor ductility at room temperature [3]. The development of Ti_3Al-base alloys calls for us to recognize the effect of microstructure on the mechanical properties in the Ti_3Al-Nb systems [4, 5]. It has been shown that the addition of Nb, Mo and V brings about the great complexity of the phase equilibrium and transformations in the Ti-Al-Nb system and results in not only ordering of the β phase but also improving the ductility to some extent [6]. Although much work on microstructure and mechanical behavior of Ti_3Al-base alloys at room temperature has been carried out, studies of high temperature deformation behavior of Ti_3Al-Nb-V-Mo alloy are seldom reported [7–10]. Williams and Blackburn [11] observed that in α_2 alloys compressed to a strain of 3%, straight screw dislocation pairs with $\vec{b}=\mathrm{a}/3\langle 11\bar{2}0\rangle$ were present on the prismatic, pyramidal and basal planes. Lipsitt *et al*. [12] found that $\vec{c}+\vec{a}/2$-type dislocations slipped on the non-basal planes during tensile deformation of the ternary Ti-26.6Al-4.94Nb alloy at 700°C, and the slip in the α_2 phase occurred on prismatic and basal planes with $\vec{b}=1/6\langle 11\bar{2}0\rangle$ between 500°C and 700°C. Court *et al*. [13] found that $\vec{a}$-type dislocations were on the basal planes in a compressed Ti-25Al-5Nb alloy at room temperature and no dislocation dissociation occurred on basal planes due to the high APB energy. Thomas *et al*. [14] and Yang [15] observed $\vec{c}$-type edge dislocations in a 4%Nb ternary alloy and suggested that the dislocations had the preferred slip planes of $\{11\bar{2}0\}$ and were sensitive to strain rate. The aim of the present work was to provide an answer to the phenomenon of ductility variation with temperature of Ti_3Al-Nb-V-Mo alloy through identifying the microstructural deformation process.

TABLE I Chemical composition of the experimental alloy

Element	Ti	Al	Nb	V	Mo
at.%	Bal.	24.0	14.0	3.0	0.5
wt.%	Bal.	15.65	31.44	3.69	1.16

2. Experimental

An ingot of the Ti-24Al-14Nb-3V-0.5Mo alloy was melted by vacuum consumable electrode arc melting. The chemical composition of the experimental alloy is presented in Table I. The ingot was first forged in the β region, and then forged in the $\alpha_2 + \beta$ region followed by air cooling (AC). Finally, these bars were cold rolled to obtain a fine-grained microstructure, and were solution treated at 1000°C for 1h followed by water quenching (WQ). The specimen was tensioned by a strain of 3% at temperatures of 27, 300, 500 and 700°C. Slices of 0.2 mm in thickness were cut perpendicular to the tensile axis from the gage length part of tensile specimens and polished mechanically to 50 μm in thickness and then electropolished to electron transparency in a twin jet electropolisher. The foils were examined in the H-800 TEM and dislocation structures were analyzed in accordance with the $\vec{g} \cdot \vec{b} = 0$ invisibility criterion in the TEM equipped with a side entry goniometer stage capable of ±45° tilt on the X or Y axis operating under two-beam conditions. Several suitable operating reflections $\vec{g}_1, \vec{g}_2 \ldots\ldots$ were chosen so as to make dislocations invisible, thus, $\vec{b} = \vec{g}_1 \Lambda \vec{g}_2$. The $\vec{b}$ direction of dislocation line can be determined according to this method, but the magnitude of $\vec{b}$ should depend on the intensity of diffraction contrast and the nature of dislocations.

3. Results and discussion

3.1. Microstructures of the alloy prior to tensile deformation

Fig. 1 shows a typical microstructure of the specimen solution treated at 1000°C for 1 hour followed by WQ before tensile deformation, which consists of the primary equiaxed α_2 phase, B_2 phase, fine plate-like O phase within α_2 grains and a small amount of residual β phase. A selected area diffraction (SAD) pattern of the α_2 phase in $[2\bar{1}\bar{1}0]$ zone axis is also shown in Fig. 1 correspondingly. Because the ductility of the solution treated specimen is higher ($\delta = 5.9\%$) than that of the aged specimen ($\delta = 1.1\%$) [16], and the α_2 and B_2 phase are main phase under solution treatment condition in the Ti_3Al-Nb-V-Mo alloy, it is necessary to investigate the microstructure of the α_2 and B_2 phase, which is useful to understand the overall microstructure and properties of the Ti_3Al–base alloy. Since the microstructural features of the B_2 phase in deformed specimen has been already studied in detail [17], the present paper focuses on the microstructural development during tensile deformation of the ordered α_2 phase.

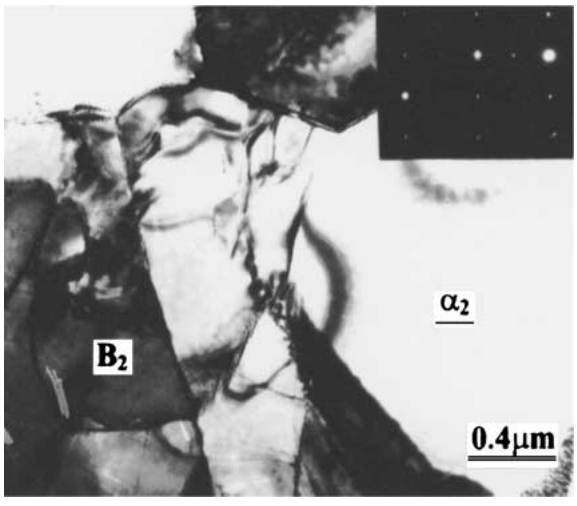

Figure 1 TEM micrograph of as-heat treated (1000°C/1h/WQ) Ti-24Al-14Nb-3V-0.5Mo alloy showing α_2 and B_2 phases.

3.2. Microstructures in room temperature tensile deformation samples

Fig. 2 shows TEM micrographs and the dislocation configurations of the alloy tensioned by 3% at room temperature. It can be seen from Fig. 2a that the α_2/α_2, α_2/B_2 and B_2/B_2 boundaries are still clear, which indicates that there is very limited deformation in the α_2 and B_2 grains. Fig. 2b shows numerous slip bands and dislocation tangles in the B_2 phase. The dislocation density in general was higher in B_2 phase than in α_2 phase, apparently due to diverse slips in the former phase.

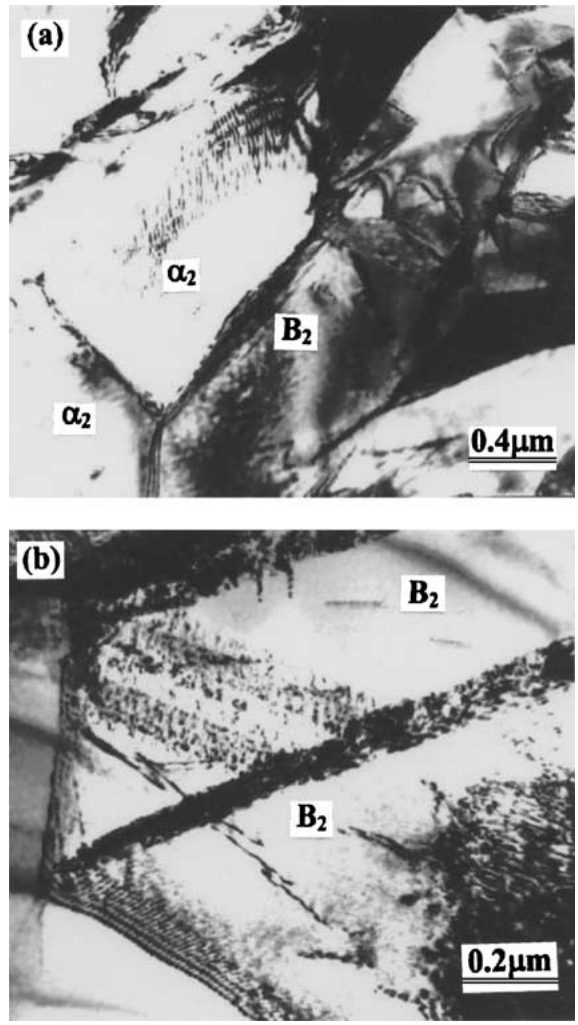

Figure 2 TEM micrographs of the Ti-24Al-14Nb-3V-0.5Mo alloy heat treated as 1000°C/1h/WQ and deformed 3% by tension at room temperature showing (a) the grain boundaries of α_2 and B_2 grains and (b) dislocation slip bands and a dislocation tangle in the B_2 grain.

The reason why the B_2 phase has a great deformation ability than the α_2 phase is that the ordered B_2 phase (bcc) has more slip systems than the ordered α_2 phase ($D0_{19}$). Moreover, the amount of B_2 phase was larger than α_2 phase in the 1000°C/1h/WQ treated specimens [16, 17]. The combined effects resulted in a greater undertaking of strains by B_2 phase than by α_2 phase during tensile deformation.

Another bright field images taken from the 1000°C/1h/WQ treated Ti-24Al-14Nb-3V-0.5Mo alloy tensioned by 3% at room temperature are shown in Fig. 3. The analysis of dislocation diffraction and diffraction contrast shows that there are $\vec{a}$-type superpartical dislocation pairs (the average width is about 20 nm) in the primary α_2 phase. While the $\vec{a}$-type dislocations with $\vec{b} = 1/6\langle 11\bar{2}0\rangle$ are superpartial, the $\vec{c}$-type dislocations with $\vec{b} = 1/3[0003]$ are not. It is deduced, therefore, the dislocation pairs shown in Fig. 3a are superpartial pairs generated from the reaction $1/3\langle 11\bar{2}0\rangle \rightarrow 1/6\langle 11\bar{2}0\rangle + 1/6\langle 11\bar{2}0\rangle$. The slip plane of dislocations can be determined not only by the nature and diffraction contrast feature of dislocation line under different operating projections but also by tilting experiments. Namely, the edge-on condition, which is to place the dislocation array to lie edge-on perpendicular to slip planes [18]. It was concluded by this method that the superpartical dislocation paris slip on prismatic planes in the α_2 grain, which is in good agreement with the results of Williams and Blackburn [11]. Fig. 3b shows some hexagonal dislocation networks at the α_2/B_2 boundary. Analysis of the trace shows that these dislocations are $\vec{a}$-type dislocations, and the distance between dislocations line along the same direction is the largest when the foil orientation is close to the [0001] zone axis, the slip plane of $\vec{a}$-type dislocations therefore is the basal plane (0001). The existence of dislocation network in the α_2 grain is considered to be a result of interaction between two arrays of dislocations of the same type. In other words, two rows of $\vec{a}$-type dislocations with an angle of 120° can react to form hexagonal networks, which can be expressed as $1/6[2\bar{1}\bar{1}0] + 1/6[\bar{1}2\bar{1}0] = 1/6[11\bar{2}0]$.

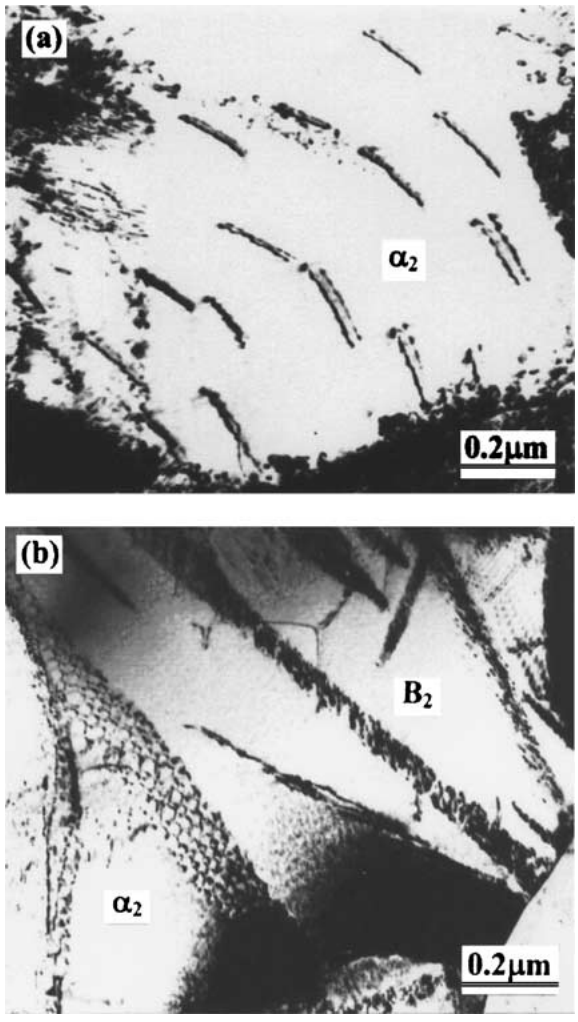

Figure 3 TEM micrographs showing microstructures of Ti-24Al-14Nb-3V-0.5Mo alloy heat-treated as 1000°C/1h/WQ and tensile deformed by 3% at room temperature: (a) $\vec{a}$-type dislocation pairs on prismatic planes in a primary α_2 grain, (b) $\vec{a}$-type dislocation networks on basal planes in the primary α_2 grain near the boundary neighboring a B_2 grain.

3.3. Microstructures in samples tensile deformed at 300°C and 500°C

Fig. 4 shows a series of dislocation images in an α_2 grain in a specimen tensile deformed at 300°C. In order to determine $\vec{b}$ of the straight dislocations, the sample stage has been tilted to different zone axes of the α_2 grain, and the operating reflections of $\vec{g} = 0\bar{2}20$, $\bar{2}020$, $\bar{1}100$, $\bar{2}022$, $\bar{2}202$, $01\bar{1}\bar{1}$ and $\bar{1}\bar{1}22$ in [0001], $[2\bar{1}\bar{1}3]$ and $[11\bar{2}3]$ zone axes have been chosen. For example, 'A' dislocations are invisible with $\vec{g} = 0\bar{2}20$ (Fig. 4b) and $\vec{g} = 01\bar{1}\bar{1}$ (Fig. 4c), but are visible with $\vec{g} = \bar{1}100$ (Fig. 4a) and $\vec{g} = \bar{2}202$ (Fig. 4d), which proves that 'A' dislocations are $\vec{a}$-type dislocations with $\vec{b} = 1/6[2\bar{1}\bar{1}0]$. 'B' and 'C' dislocations were analyzed similarly. The slip plane was determined by means of nature of dislocation diffraction contrast and morphology feature in the different slip planes. Generally speaking, $\vec{a}$-type dislocations usually slip on prismatic planes $\{10\bar{1}0\}$ in the form of single dislocation line or superpartial dislocation pairs and form hexagonal dislocation networks on basal planes (0001). As for $\vec{c} + \vec{a}/2$-type dislocations, they usually occur on pyramidal planes as superpartical dislocation pairs [19]. Therefore, it is determined that 'A', 'B' and 'C' dislocations were $\vec{a}$-type dislocations on prismatic planes $\{10\bar{1}0\}$.

The dislocation structures in specimens deformed at 500°C showed the same slip planes, $\{10\bar{1}0\}$, as those of the specimens deformed at 300°C. Fig. 5 shows the typical dislocation structures obtained by tensile deformation at 500°C. The distribution of dislocations were similar to the case of 300°C deformation. There were both straight dislocations and hexagonal dislocation networks (marked as A and B in Fig. 5a). Varying the amount of deformation at 500°C unaffected the basic features of dislocations. However, dislocation density increased and the dislocation lines became gradually curved with increased amount of deformation, which indicated more cross slips. Through a series of diffraction analyses, it was determined that the majority of dislocations in the primary α_2 phase were of $\vec{a}$-type activated on prismatic and the basal planes. Therefore, the slip systems were not changed by increasing the deformation temperature from 300°C to 500°C.

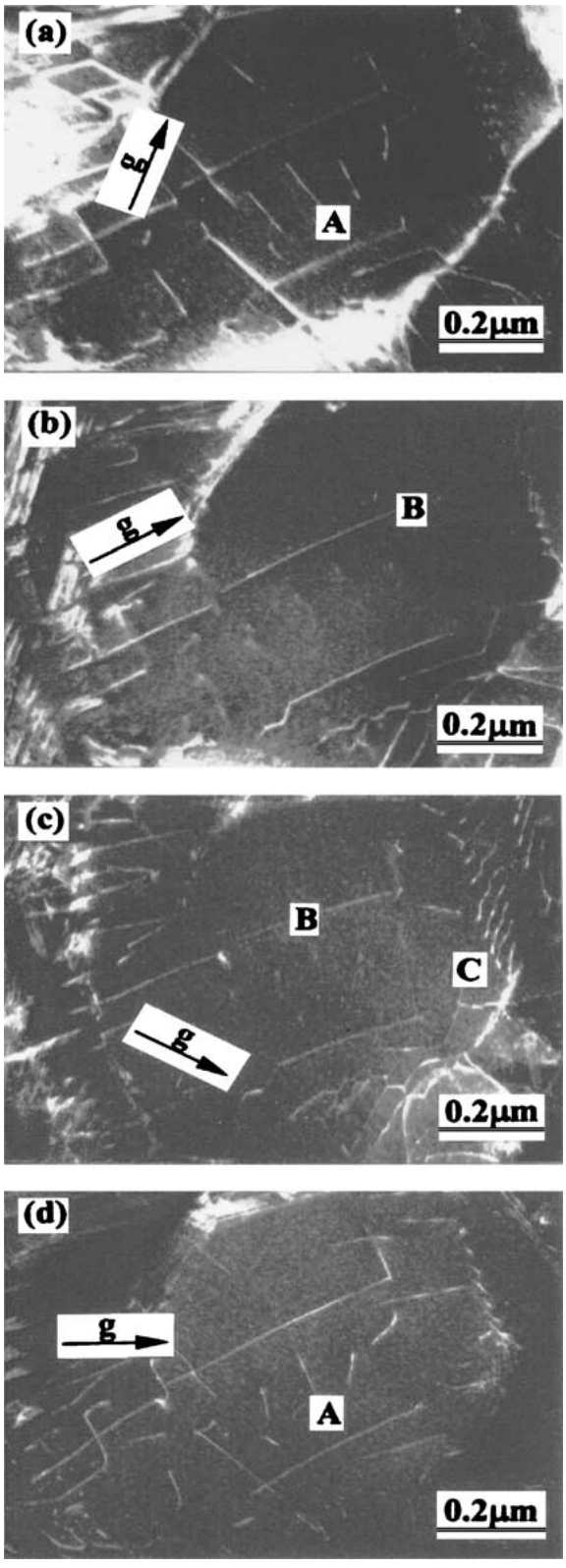

Figure 4 TEM micrographs showing dislocation structures in a primary α_2 grain in the 1000°C/1h/WQ treated Ti-24Al-14Nb-3V-0.5Mo alloy tension deformed by 3% at 300°C under different diffracting conditions: (a) $\vec{g} = \bar{1}100$; (b) $\vec{g} = 0\bar{2}20$; (c) $\vec{g} = 01\bar{1}\bar{1}$ and (d) $\vec{g} = \bar{2}202$.

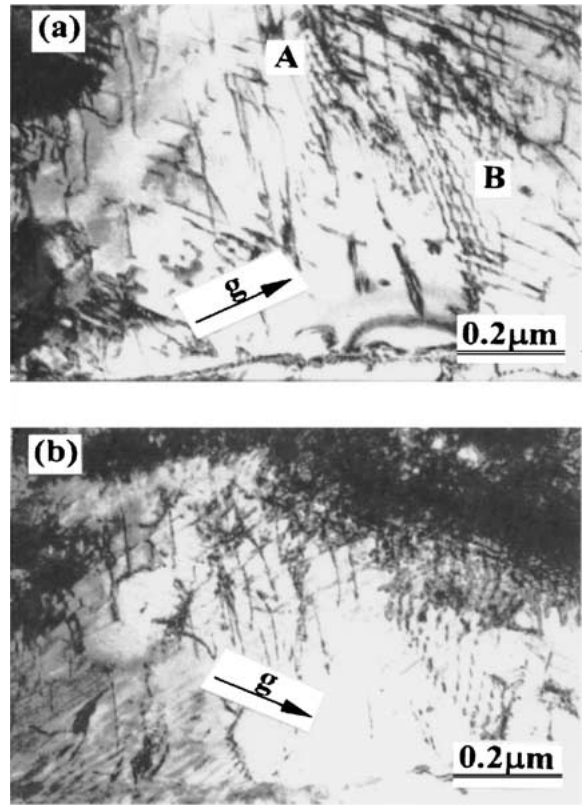

Figure 5 TEM micrographs showing dislocation structures in a primary α_2 grain in Ti-24Al-14Nb-3V-0.5Mo alloy heat treated as 1000°C/1h/WQ and tensile deformed by 3% at 500°C under different diffracting conditions: (a) $\vec{g} = \bar{1}100$ and (b) $\vec{g} = \bar{1}011$.

3.4. Microstructures in samples tensile deformed at 700°C

Fig. 6 shows TEM micrographs in the Ti-24Al-14Nb-3V-0.5Mo alloy in 700°C tensile deformed samples. Comparing the variation of samples tensioned at different temperatures (Fig. 1, Fig. 2a and Fig. 7a), it is clear that microstructures became finer and the α_2/α_2 and α_2/B_2 boundaries were vague when the alloy was deformed at this high temperature. It is known from the Ti_3Al-Nb pseudo-binary phase diagram that 700°C corresponds to the $\alpha_2 + O$ two-phase region [20]. The previous investigation [16, 17] identified a considerable amount of secondary acicular α_2 phase precipitation from the B_2 matrix and the O phase from the primary α_2 phase when the Ti_3Al-Nb-V-Mo alloy was deformed at this temperature. The result was that the primary and secondary acicular α_2 phase had higher volume fraction than the B_2 phase and the deformation of the alloy was concentrated on the α_2 grains. Also, dynamic recovery could occur during deformation at 700°C. Evidences of recovery and recrystallization were found, an example of the latter as shown in Fig. 6b. In addition, as that shown in Fig. 6c, the curved dislocations are the main feature in the α_2 phase, which testified that slip and cross-slips were promoted. Like the other cases, the image analysis with varying diffraction conditions was conducted. Especially with $\vec{g} = 0002$, in which most of dislocations were invisible, it was deduced that $\vec{a}$-type dislocations were of the major type and there were only a few $\vec{c} + \vec{a}/2$-type dislocations, and no $\vec{c}$-type dislocation was found. From the fact that the slip planes of $\vec{c} + \vec{a}/2$-type dislocations are usually pyramidal planes $\{20\bar{2}1\}$ [18], it was concluded that $\vec{a}$-type and $\vec{c} + \vec{a}/2$-type dislocations slips were the main deformation modes of the Ti_3Al-Nb-V-Mo alloy at high temperature.

As is well known, in polycrystalline hcp metals, basal slips and prismatic plane slips do not supply sufficient slip modes to satisfy Von Mises' criterion

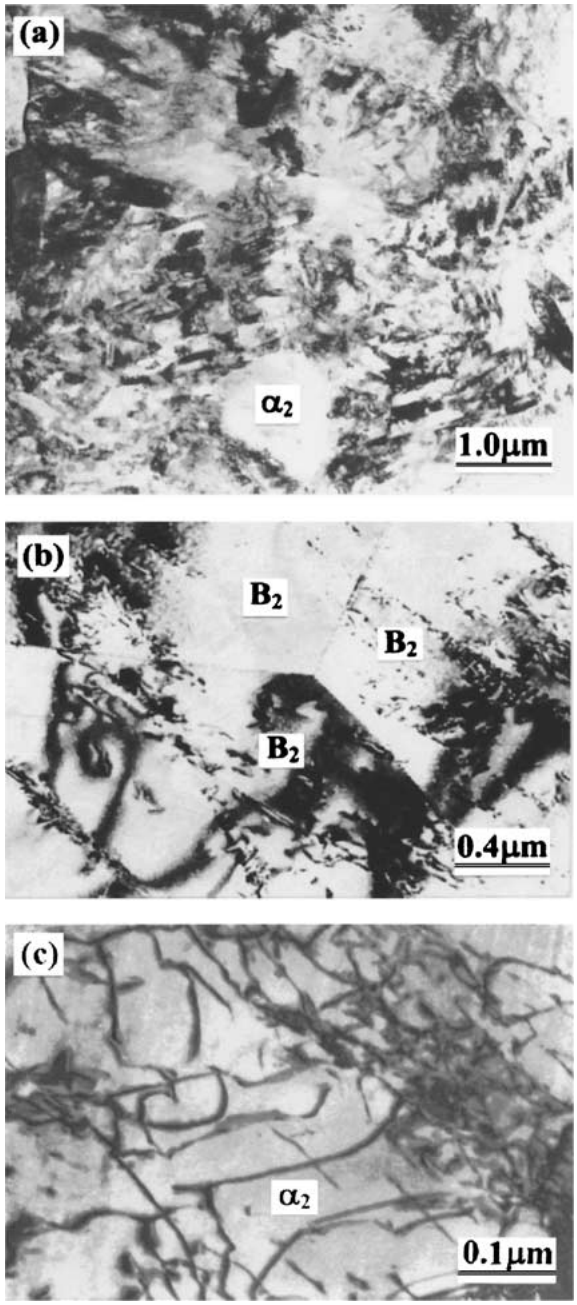

Figure 6 TEM micrographs showing microstructures of Ti-24Al-14Nb-3V-0.5Mo alloy heat treated as 1000°C/1h/WQ and tensile deformed by 3% at 700°C: (a) refined microstructure with vague grain boundaries, (b) an area of recrystallized B_2 grains and (c) curved dislocations in the α_2 phase.

which states that every grain should be able to plastically deform generally to meet the shape changes imposed by its neighbors. Consequently, twinning and occasionally other slip systems play an important role in the plasticity of hcp structure metals. As for the intermetallics with ordered $D0_{19}$ crystal structure, there is a relationship between the lattice parameters in the ordered state and those in the disordered hcp state such that $a_{D019} = 2a_{hcp}$, $c_{D019} = c_{hcp}$. Therefore, the slip systems of $D0_{19}$ structure intermetallics at room temperature are usually considered to be $\{10\bar{1}0\}\langle 0001\rangle$, $\{10\bar{1}0\}\langle 11\bar{2}0\rangle$, $\{0001\}\langle 11\bar{2}0\rangle$, $\{20\bar{2}1\}\langle 11\bar{2}6\rangle$ and $\{20\bar{2}1\}\langle 11\bar{2}0\rangle$ in the order of activity. Since the lattice ratio of the parameters, c/a, of α_2 phase (0.801) deviates from the ideal value (1.633), the slip systems change from the case of random hcp of the ideal case, which can be confirmed by the Peierls Nabarro (P-N) model. The critical shear stress (P-N force) of dislocation glide needed to overcome the lattice force can be expressed as [21]:

$$\sigma_c = \frac{2\mu}{1-\upsilon} \exp\left(-\frac{2\pi}{1-\nu} \times \frac{\delta}{b}\right)$$

where μ is the shear modulus, ν is the Poisson's ratio, δ is the slip distance and b is interatomic distance along the slip direction. According to this relation, the bigger the δ/b value is, the smaller the σ_c value is and the easier the dislocation glide is. The calculation showed that the δ/b of $\{10\bar{1}0\}\langle 11\bar{2}0\rangle$ slip systems was 0.58 and it was the biggest value in all of the slip systems of the α_2 phase. It is noted that the $\vec{c}$-type dislocation was not found in the present alloy. Therefore, the theoretical calculation matches the test results. That is to say, $\vec{a}$-type dislocations gliding on prismatic planes $\{10\bar{1}0\}$ are most active in the primary α_2 phase in the Ti_3Al-Nb-V-Mo alloy under room temperature tensile deformation condition.

In addition, the relationship between the P-N force and temperature can be expressed as [22]:

$$\sigma_{cT} = \sigma_c \exp\left[\sqrt{2}b^3(\mu\sigma_c)^{1/2}kT - 1/A\right]$$

where $A = f(\sigma_c, \varepsilon)$, k is the Boltzmann's constant and σ_{cT} is the P-N force when temperature is T. For the case of the $\vec{a}$-type dislocation pairs, σ_{cT} decreases sensitively with temperature due to the large Burgers vector, 0.579 nm. On the other hand, the temperature dependence of the P-N force of the $\vec{c}+\vec{a}/2$-type dislocation pairs is comparatively small because of the small Burgers vector, 0.544 nm. This explains why the $\vec{a}$-type dislocations were dominantly activated at high temperature. In summary, the $\vec{a}$-type dislocations predominantly undertake the plastic strain of α_2 phase regardless of the deformation temperature.

4. Conclusions

1. At the lower deformation temperature, $\vec{a}$-type dislocations in the primary α_2 phase not only formed hexagonal dislocation networks on basal plane (0001): $1/6[2\bar{1}\bar{1}0] + 1/6[\bar{1}2\bar{1}0] = 1/6[11\bar{2}0]$, but also dissociated into superpartial dislocation pairs on prismatic planes $\{10\bar{1}0\}$: $1/3\langle 11\bar{2}0\rangle \rightarrow 1/6\langle 11\bar{2}0\rangle + 1/6\langle 11\bar{2}0\rangle$. Being immobile, the dislocation networks were thought to be mainly responsible for the low ductility at low temperature.

2. With increasing the deformation temperature, a considerable amount of sub-grains made the microstructure finer, which was the result of dynamic recovery and precipitates of the secondary acicular α_2 phase and O phase at high deformation temperature. These microstructural developments were thought to be beneficial for the ductility at elevated temperatures.

3. In the range of room temperature to 700°C tension deformation, the slip of $\vec{a}$-type dislocations is the main deformation mode in the α_2 grain. When deformation temperature was increased up to 700°C, networks of hexagonal dislocation apparently decreased and a few

of $\vec{c}+\vec{a}/2$-type dislocations also have been found. No $\vec{c}$-type dislocations are observed.

References

1. H. A. LIPSITT, in "High Temperature Ordered Intermetallic Alloys," edited by C. C. Koch, C. T. Liu and N. S. Stoloff (MRS, Pittsburgh, 1985) p. 351.
2. A. H. ROSENSTEIN, *Mater. Sci. Eng.* **A143** (1991) 31.
3. H. A. LIPSITT, *Mat. Res. Soc. Symp. Proc.* **228** (1993) 119.
4. K. MURALEEDHARAN, A. K. GOGIA, T. K. NANDY and D. BANERJEE, *Metal. Trans.* **A23** (1992) 401.
5. J. K. NACK, J. Y. KIM and W. S. CHO, *ibid.* **A24** (1993) 1785.
6. S. M. L. SASTRY and H. A. LIPSITT, in "Ti'80, Science and Technology," edited by H. Kimura and O. Izumi (TMS-AIME, Warrendale, PA, 1980) p. 1231.
7. A. K. GOGIA, D. BANERJEE and D. NANDY, *Metall. Trans.* **A21** (1990) 609.
8. Z. CHEN and M. T. COPE, *Mater. Sci. Tec.* **8** (1992) 729.
9. Y. WU, D. Z. YANG and G. M. SONG, *Intermetallics* **8** (2000) 629.
10. B. WANG, T. JIA, D. ZOU, H. MA and Z. ZHONG, *Mater. Sci. Eng.* **A153** (1992) 422.
11. J. C. WILLIAMS and M. J. BLACKBURN, "Ordered Alloys" (Baton Rouge, Claitor's Publishing Division, 1970) p. 425.
12. H. A. LIPSITT, D. SCHECHTMAN and SCHAFRIK, *Metall. Trans.* **A11** (1980) 1369.
13. S. A. COURT, M. H. LOREJTW and H. L. FRASBR, *Scr. Metall.* **21** (1987) 997.
14. M. THOMAS, A. VASSEL and P. VEYSSIERE, *Phil. Mag.* **A59** (1989) 1013.
15. W. J. S. YANG, *Metall. Trans.* **A13** (1982) 324.
16. Y. WU, Z. X. TANG, D. Z. YANG and D. M. LI, *Materials Science Technology* (in chinese) **4** (1996) 24.
17. Y. WU and D. Z. YANG, *Journal of Harbin Institute of Technology* (in chinese) **29** (1997) 119.
18. S. C. WANG, C. Z. LI, M. G. YAN, Y. GAO and C. X. CAO, in "Intermatallics," edited by Z. Y. Zhong and H. Q. Ye (Mechanical Industry Publishing House, Beijing, China, 1992) p. 112.
19. F. S. SUN, W. GAO and C. X. CAO, *Acta Metallurgica Sinica.* **A30** (1994) 507.
20. Y. W. KIM and F. H. FROES, *Physical Metallurgy of Titanium Aluminides*, YWK1/KAS/TES **28** (1989) 203.
21. F. R. N. NABARRO, "Dislocations in Solids" (North-Holland Publishing Company, 1979) p. 168.
22. M. YAMAGNCHI and Y. UMAKOSHI, *Prog. Mater. Sci.* **34** (1990) 148.

Received 23 August 2000
and accepted 8 August 2001